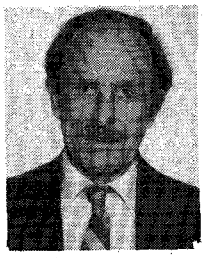

Jose Perini (M'61–SM'76) was born in São Paulo, Brazil. He received the B.S. degree in electrical and mechanical engineering from Escola Politecnica de São Paulo, São Paulo, Brazil, in 1952.

Subsequently, he worked for Real Transportes Aeroes, a Brazilian airline company, for three years, as Manager for Radio Maintenance, and in the last six months, as Assistant to the Manager of General Maintenance. In 1955 he joined the Electrical Engineering Department of Escola Politecnica de São Paulo, as an Assistant Professor, teaching until 1958. During this time, he also conducted ionospheric research. He received the Ph.D. degree in electrical engineering from Syracuse University, Syracuse, NY, in 1961. From 1959 to 1961, while studying at Syracuse, he was also a consultant for General Electric (G.E.) Co. in the Television Transmitting Antenna area. His Ph.D. dissertation was derived from this work. In 1961 he returned to Brazil as an Associate Professor of Electrical Engineering at Escola Politecnica de Sao Paulo and also as a consultant for G.E. of Brazil. In September 1962 he became Assistant Professor of Electrical Engineering at Syracuse University, where he was promoted to Associate Professor in 1966 and to Professor in 1971. He rejoined G.E. in Syracuse as a consultant in the same area of TV transmitting antennas until 1969. He has had many research contracts with the Navy, Air Force, and Army. He has consulted extensively in the U.S. and abroad in the areas of electromagnetics and communications. He has many published papers in the fields of antennas, microwaves, EMC, and circuit theory. He also holds two patents on TV transmitting antennas.

Optical Control of GaAs MESFET's

ALVARO AUGUSTO A. DE SALLES

Abstract—**Theoretical and experimental work for the performance of GaAs MESFET's under illumination from light of photon energy greater than the bandgap of the semiconductor is described. A simple model to estimate the effects of light on the dc and RF properties of MESFET's is presented. Photoconductive and photovoltaic effects in the active channel and substrate are considered to predict the change in the dc equivalent circuit parameters of the FET, and from these the new Y- and S-parameters under illumination are calculated. Comparisons with the measured S-parameters without and under illumination show very close agreement.**

Optical techniques can be used to control the gain of an FET amplifier and the frequency of an FET oscillator. Experimental results are presented showing that the gain of amplifiers can be varied up to around 20 dB and that the frequency of oscillators can be varied (tuning) around 10 percent when the optical absorbed power in the active region of the FET is varied by a few microwatts.

When the laser beam is amplitude-modulated to a frequency close to the free-running FET oscillation frequency, optical injection locking can occur. An analytical expression to estimate the locking range is presented. This shows a fair agreement with the experiments. Some suggestions to improve the optical locking range are presented.

I. Introduction

IN THE LAST FEW YEARS, an increasing interest has been shown on the possibilities of using the light effects to control the various functions of the FET's. Conventional methods of MESFET amplifier and oscillator control involve direct electrical connection of the control source to the device. However, in optical control, light provides the coupling medium, allowing the control signal to be distributed using optical fiber technology. This offers considerable advantages, particularly where electrical isolation and immunity from electromagnetic interference are important requirements.

The injection of light provides effectively an extra terminal to the device, which possesses inherent optical isolation, no decoupling structures being required. These decoupling structures are very often undesired because they are usually lossy and their dimensions can be unsuitable for the miniaturization required. Also, in the near infrared region (photon energies close to the GaAs bandgap) the optical absorption depths in GaAs are of the order of 1 μm, therefore being compatible with the microwave device structures.

Some experiments have shown that the FET dc characteristics may alter with illumination [1] and that FET oscillators may be tuned by varying the intensity of the light falling on the active region of the device [2]. Also, some authors [3]–[5] have recently reported high-speed optical detection with GaAs MESFET's.

The present work has been developed elsewhere [6] in more detail. Only commercially available GaAs MESFET's were used, providing therefore very poor coupling efficiency between optical and microwave energies due to the small active region available for optical absorption. However, since more and more systems are using optical transmission, direct optical interfaces become very attractive. Thus future development with a modification of the present available device structure for optimum optical/microwave interaction is likely.

The fundamental physical mechanism arising in optical illumination of the MESFET is the production of free carriers (electron-pairs) within the semiconductor material when light of photon energy equal to or greater than the semiconductor bandgap energy is absorbed. Gaps between

Manuscript received February 7, 1983; revised April 2, 1983. This work was supported in part by the U.K. Science Research Council, the U.K. Ministry of Defense (A.S.W.E.), and the CNP_q (Brasil).

The author is with Centro de Estudos em Telecommunicações (CETUC), PUC/RJ, Rua Marquês de São Vincente, 225-Rio de Janeiro-RJ, BRASIL.

0018-9480/83/1000-0812$01.00 ©1983 IEEE

gate and source and between gate and drain allow penetration of light, which is absorbed in the active region, buffer layer (if present), and substrate. Photovoltaic effects in the gate Schottky-barrier region and in the active channel to substrate (or buffer layer) barrier occur, as well as photoconductive effects in the parasitic resistances in series with the active channel and in the substrate (and buffer layer, if present). These change the relevant parameters of the device, such as the transconductance, the gate-to-source capacitance, and the drain-to-source resistance. When the external circuits are correctly designed, these changes can be enhanced to provide useful modification of the MESFET terminal characteristics.

A full solution of the continuity equations in the various regions would describe in detail the photoeffects. This can be done using a two-dimensional numerical simulation, but usually it is a formidable task and gives little physical insight. Rather than that, the dc and RF properties of the MESFET under illumination are estimated from the introduction of the photovoltaic and photoconductive effects in the well-established theory for the MESFET without illumination [7]–[9]. Equivalent circuit elements and the associated *Y*- and *S*-parameters under illumination are predicted. These, together with conventional microwave circuit techniques, are used to estimate the performance of MESFET amplifiers and oscillators under illumination.

Some results of the experimental work carried out to assess the effects of illumination in the control of the relevant functions of the device, namely the gain of FET amplifiers, the frequency tuning, and the phase locking (synchronization) of FET oscillators, are presented. The control of the gain of FET amplifiers and of the frequency of FET oscillators is obtained by varying the intensity of a CW optical signal absorbed in the active region of the device. The phase locking of FET oscillators occurs when an optical signal, amplitude modulated at a frequency close to the free-running frequency of the oscillator, is absorbed in the active region of the device.

Finally, suggestions for new FET structures and a discussion of potential systems applications are presented.

II. Photovoltaic and Photoconductive Effects in the MESFET's

The major contribution to the gate circuit photocurrent in the MESFET's is due to holes generated in the depletion region and to those generated in the undepleted region and diffusing to the depletion region before they recombine. The FET structure is reasonably complex, but considering some simplifications, the following expression is obtained for the gate photocurrent density [6]:

$$J_{ph} = q(1-R)\phi_0\left[\frac{\alpha^3 L_p^2 w_n e^{-\alpha w}}{d^2 L_p^2 - 1} + \alpha w\right] \qquad (1)$$

where

- q electronic charge,
- R reflectivity of the surface,

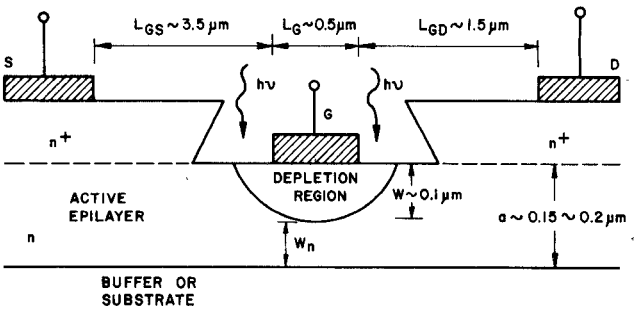

Fig. 1. Schematic geometry for the estimation of the photocurrent in the MESFET.

TABLE I
Typical Parameters for the FET Used in the Experimental Work

L_G	$= 0.5\mu m$	v_s	$= 0.9 \times 10^7$ cm/s
L_{GS}	$= 3.5\mu m$	E_s	$= 3$ kV/cm
L_{GD}	$= 1.5\mu m$	V_{bi}	$= 0.76$V
a	$= 0.15\mu m$	$\varepsilon_r\varepsilon_0$	$= 1.1 \times 10^{-12}$ F/cm
Z	$= 300\mu m$	N_{sub}	$= 10^{13}$ cm^{-3}
N_D	$= 1.5\times10^{17}$ cm^{-3}	L_p	$= 2\mu m$
μ_n	$= 4500$ cm^2/V.	τ_p	$= 10^{-9}$ s
		τ_n	$= 10^{-6}$ s

- ϕ_0 photon flux density per second at the surface,
- α optical absorption coefficient,
- L_p minority-carrier (hole) diffusion length,
- w_n width of the undepleted region,
- w width of the depletion region.

Typical parameters for the FET[1] used in the experimental work are shown in Table I.

Fig. 1 illustrates the schematic geometry of the MESFET under illumination from the top.

A CW double-heterostructure GaAs/Ga AlAs stripe-geometry laser diode (ITT type LS 7709) was used in most of the experiments. A simple optical focusing system using an Ealing microscope objective (type 24-9797, ×20 amplification and 0.54 numerical aperture) is used. This gives average beam diameters measured (using a Fairchild CCD array, type CCD133) in the range 50–150 μm, depending on the adjustment of the relative positions of laser, objective, and focal plane. For the levels of illumination used in the experiments (laser output power around 2 mW focused to a 50-μm spot), (1) gives a photocurrent density of the order of 10^5 A/m^2, which in an effective area of semiconductor of 10^{-10}m^2 contributing to the photocurrent gives

$$I_{ph} = J_{ph} \times A_{\text{eff}} = 10^{-5} A.$$

This predicted photocurrent ($\cong 10\ \mu$A) is in a fair agreement with the experiments (Fig. 2).

[1]GAT 6 GaAs MESFET's (package P-109) from Plessey.

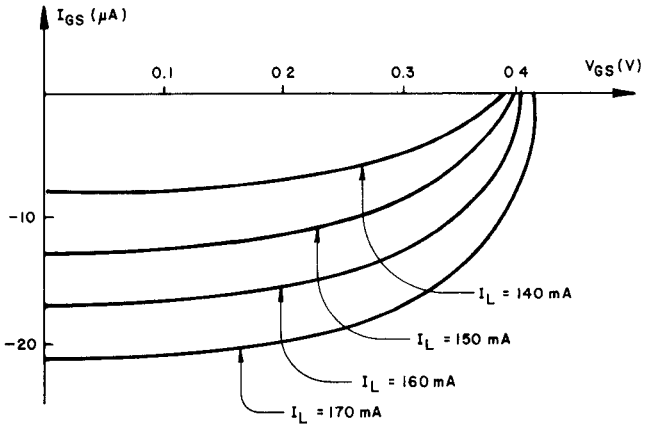

Fig. 2. Measured current–voltage characteristics of the Schottky-barrier gate junction of the GAT 6 GaAs MESFET under illumination (I_L is the laser drive current, Fig. 3).

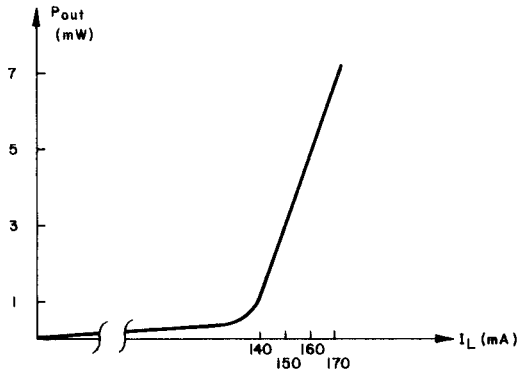

Fig. 3. Laser diode (ITT LS 7709) output power versus drive current characteristic.

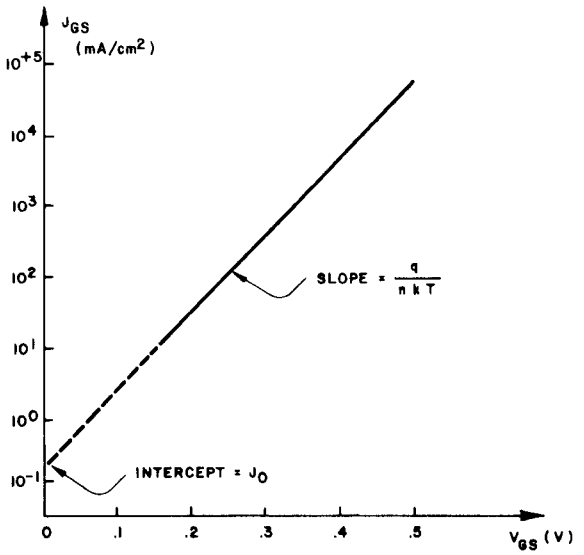

Fig. 4. Forward characteristic of the Schottky-barrier junction.

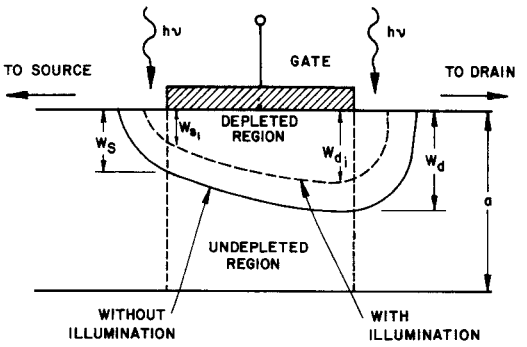

Fig. 5. Schematic diagram of the active channel profile with --- and without —— illumination.

Fig. 2 shows the current–voltage characteristics of the GAT 6 GaAs MESFET Schottky-barrier junction measured under different illumination levels. Fig. 3 illustrates the laser diode power output versus drive current characteristic.

The current–voltage characteristics of the Schottky junction under illumination is [10]

$$J = J_s e^{qv/nkT} - J_{ph} \tag{2}$$

where J_s is the saturation current density and n is the ideality factor. An approximate value for the parameters J_s and n can be obtained from the measured current–voltage forward characteristic of the Schottky-barrier junction (Fig. 4).

Using this technique, values of $n \sim 1.4$ and $J_s \sim 0.2$ mA/cm^2 are estimated. For a short-circuit photocurrent of the order of 10 μA, an open-circuit photovoltage around 0.4 V is measured (Fig. 2), which is in close agreement with the 0.39 V obtained using (2)

$$V_{oc} = \frac{nkT}{q} \ln \frac{J_{sc}}{J_s}. \tag{3}$$

Since the photovoltage developed across the Schottky barrier is known, its introduction in some simple analytical models for the FET under dark conditions [7]–[9] enables us to estimate the change of the FET basic parameters due to the photovoltaic effect, such as the gate capacitance, opening of the active channel, and transconductance.

Fig. 5 illustrates the change in the depleted–undepleted boundary profile due to the photovoltaic effect in the gate depletion region of the MESFET.

Following [7] and [8], the reduced "potentials" under illumination

$$t_i = \frac{w_{s_i}}{a} = \sqrt{\frac{V_S + V_{bi} - V_{GS} - V_{ph}}{V_{po}}} \tag{4}$$

and

$$u_i = \frac{w_{d_i}}{a} = \sqrt{\frac{V_D + V_{bi} - V_{GS} - V_{ph}}{V_{po}}} \tag{5}$$

in the source and drain ends of the active channel are introduced. Here

V_{ph} photovoltage developed across the junction ($V_{ph} \geqslant 0$),

V_S voltage at the source end of the gradual channel,
V_D voltage at the drain end of the gradual channel,
V_{bi} gate junction built-in potential,
V_{GS} gate-to-source bias voltage ($V_{GS} \leqslant 0$),
w_{s_i} opening of the active channel in the source end of the active channel,
w_{d_i} opening of the active channel in the drain end of the active channel,
a thickness of the epilayer
and

$$V_{po} = \frac{q \cdot N_d \cdot a^2}{2\epsilon_0 \epsilon_r} \tag{6}$$

is the pinchoff potential. The voltages $V_S + V_{bi} - V_{GS} - V_{ph}$ and $V_D + V_{bi} - V_{GS} - V_{ph}$ are the total channel-to-gate potential in the source and drain ends of the gradual channel, respectively. When saturation drift velocity occurs, $V_D = V_{\text{sat}}$ and $u_i = u_{im}$. The quantity $a\,(1 - u_{im})$ is a measure of channel opening at saturation.

Therefore, following an analysis similar to that applied to the MESFET without illumination, analogous expressions are found for the active channel behavior. Actually, the photovoltage V_{ph} developed is superimposed on the gate bias voltage V_{GS}, the active channel parameters changing accordingly.

Then, the channel current is [7], [6]

$$I_{\text{chi}} = \frac{g_o V_{po}}{3}\left[\frac{3\left(u_i^2 - t_i^2\right) - 2\left(u_i^3 - t_i^3\right)}{1 + z\left(u_i^2 - t_i^2\right)}\right] \tag{7}$$

where

$$g_0 = \frac{q \cdot N_d \cdot \mu_n \cdot a \cdot Z}{L_G} \tag{8}$$

is the open-channel conductance and

$$z = \frac{\mu_n \cdot V_{po}}{v_s \cdot L_G} \tag{9}$$

is a reduced velocity. Here, v_s is the majority-carrier saturation drift velocity, μ_n is the majority-carrier mobility, and L_G and Z are the length and width of the gate, respectively.

Photoconductive effects in the resistances associated with the FET equivalent model are calculated using the dark values given in [11]. For the levels of illumination used in the experiments, a decrease of around 10 percent in the parasitic resistances in series with the active channel is obtained.

Fig. 6 illustrates comparisons between predicted and measured $I-V$ characteristics for the MESFET with and without illumination. A fair agreement is achieved with this simplified model.

When a high external resistance ($R_G > 50$ kΩ) is connected to the gate circuit, the gate junction under illumination operates near to its open-circuit condition, the photovoltage developed being close to V_{oc}. This is superimposed on the reverse gate bias V_{GS} and the overall effect is that the gate depletion region is "pinned" to a forward bias near to V_{oc} (~ 0.38 V). This is shown in Fig. 7.

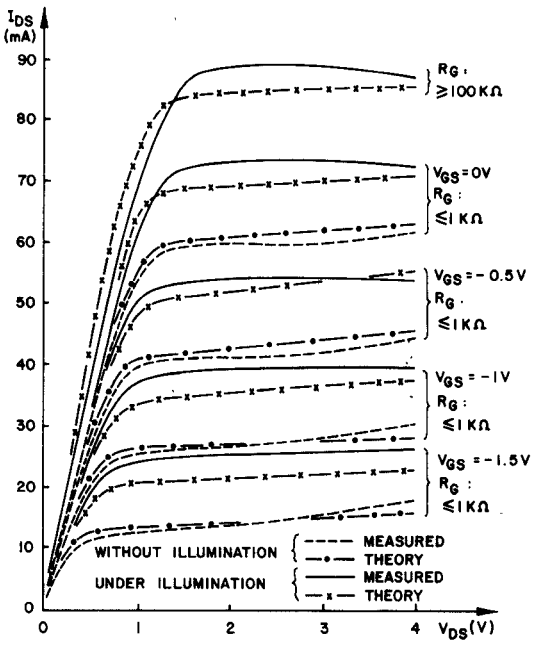

Fig. 6. Theoretical and measured $I-V$ characteristics of GAT 6 GaAs MESFET with and without illumination (laser drive current I_L = 155 mA, $V_{oc} \sim 0.4$, $I_{SC} \sim 15$ μA).

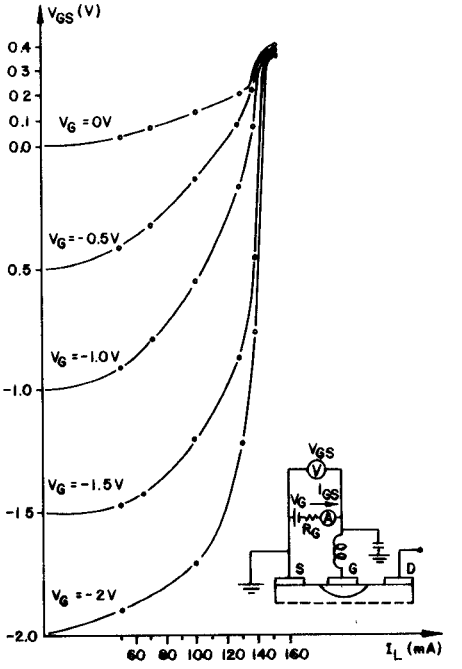

Fig. 7. Schottky-barrier photovoltage versus laser drive current for different gate bias V_G (R_G = 1 MΩ).

III. RF Performance Under Illumination

A simplified circuit model for the MESFET [12], [6] in the common-source configuration under illumination is used (Fig. 8).

It is adopted similar representation as for the solar cell model to account for the photovolatic effect, the current sources producing the same current as the photocurrent associated with the correspondent depletion layer.

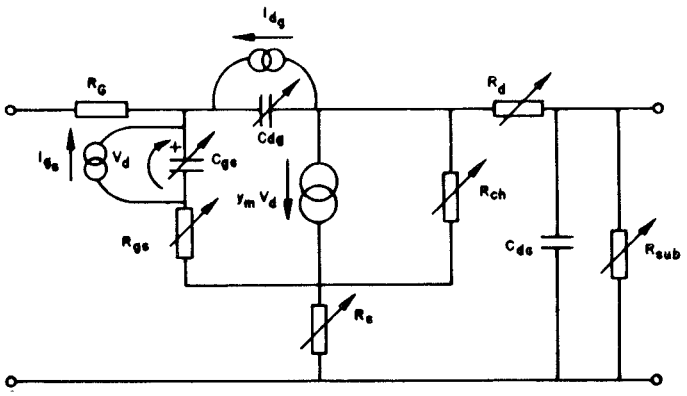

Fig. 8. Small signal equivalent circuit for the intrinsic MESFET under illumination.

Lumped circuit elements have physical origins within the device

- C_{gs} gate-to-channel depletion capacitance,
- R_{gs} charging channel resistance to C_{gs},
- C_{dg} drain-to-gate feedback capacitance,
- y_m transadmittance of magnitude g_{mo} and phase delay τ reflecting delay between input and output signals,
- R_{ch} channel resistance,
- R_s source-to-channel resistance,
- R_d drain-to-channel resistance,
- R_g gate–metal resistance,
- C_{ds} drain-to-source capacitance,
- R_{sub} substrate resistance.

When the change in the equivalent circuit parameters due to the photovoltaic and photoconductive effects is estimated, Y- and S-parameters of the intrinsic device are calculated from usual relationships [12], [13].

The transconductance in the saturation region under illumination is found to be [7], [6]

$$g_{m_i} = g_o \frac{u_{m_i} - t_i}{1 + z\left(u_{m_i}^2 - t_i^2\right)}. \tag{10}$$

For short gate devices ($L_G/a \leqslant 5$) and when the voltage $V_{bi} - V_{GS} - V_{ph}$ in the gate is not too near the pinchoff value V_{po}, the gate-to-source capacitance under illumination is given by [9], [6]

$$C_{gs_i} \cong 2\epsilon_o \epsilon_r Z \left[\frac{L_G}{a \cdot u_i} + 1.56\right]. \tag{11}$$

Simple computer programs [6] are used to calculate the FET equivalent circuit parameters from the S-parameters and vice versa. S-parameters with and without illumination are measured and compared with the estimated.

Tables II and III show the measured S_{21} parameter for the GaAs MESFET with and without illumination for gate bias voltages of 0 V and -1 V, respectively. External gate resistance R_G is changed from 1 kΩ to 1 MΩ to show

TABLE II
SMALL SIGNAL S_{21}-PARAMETER WITH AND WITHOUT ILLUMINATION FOR HIGH (1 MΩ) AND LOW (1 kΩ) GATE LOAD RESISTANCES
$V_{GS} = 0$ V.

	R_G = 1KΩ				R_G = 1MΩ			
	AMBIENT		ILLUMIN.		AMBIENT		ILLUMIN.	
FREQ (GHz)	MAG	PHASE	MAG	PHASE	MAG	PHASE	MAG	PHASE
2	2.40	141	2.40	141	2.57	140	2.63	138
3	2.24	120	2.24	120	2.24	120	2.32	119
4	2.40	99	2.40	99	2.43	99	2.54	97
5	2.29	81	2.29	81	2.32	81	2.37	79
6	2.34	63	2.32	63	2.29	63	2.34	61
7	1.97	53	1.97	53	2.00	53	2.02	51
8	1.55	30	1.55	30	1.57	30	1.58	28
V_G	- 0.02V		- 0.02V		+ 0.06V		+ 0.33V	
I_{DS}	69mA		79mA		68mA		85mA	
I_{GS}	0.2μA		-3.5μA		0.0μA		- 0.2μA	

TABLE III
SMALL SIGNAL S_{21}-PARAMETER WITH AND WITHOUT ILLUMINATION FOR HIGH (1 MΩ) AND LOW (1 kΩ) GATE LOAD RESISTANCES
$V_{GS} = -1$ V.

	R_G = 1KΩ				R_G = 1MΩ			
	AMBIENT		ILLUMIN.		AMBIENT		ILLUMIN.	
FREQ. (GHz)	MAG	PHASE	MAG	PHASE	MAG	PHASE	MAG	PHASE
2	2.37	133	2.37	133	2.34	133	2.60	132
3	2.19	117	2.19	117	2.16	116	2.40	115
4	2.26	110	2.26	110	2.32	100	2.57	97
5	2.24	83	2.24	83	2.21	81	2.43	78
6	2.07	66	2.07	65	2.11	67	2.29	64
7	1.80	54	1.80	54	1.80	54	1.97	51
8	1.48	29	1.48	29	1.48	28	1.64	25
V_G	- 1V		- 0.98V		- 1V		- 0.23V	
I_{DS}	38mA		46mA		39mA		69mA	
I_{GS}	-4μA		-9.7μA		-4.0μA		- 4.7μA	

the significant influence of the photovoltage developed in the gate junction. It is seen that the major variation in the S_{21}-parameters with illumination occurs when a high resistance ($R_G = 1$ MΩ) is connected to the gate circuit. The gate junction operates near the open-circuit condition with a photovoltage (close to $V_{oc} \sim 0.4$ V) forward biasing the Schottky junction. The transconductance of the device is therefore increased. No significant variations were observed in the S_{11}, S_{12}, and S_{22} parameters under similar conditions.

From the measured S-parameters with and without illumination, with high ($R_G = 1$ MΩ) and low ($R_G = 1$ kΩ) gate resistances, the FET equivalent circuit parameters are calculated. It was noticed that the transconductance g_m and the gate-to-source capacitance C_{gs} have a significant

increase (10 to 20 percent) with illumination only when the gate resistance is high ($R_G = 1$ MΩ), in agreement with the previous observations.

The changes of the transconductance and of the gate-to-source capacitance of the device with illumination can, therefore, be predicted and measured, and this is now used to estimate the performance of FET amplifiers and oscillators under illumination.

IV. Control of the Gain of MESFET Amplifiers

The change in the transconductance of the device with illumination can be used to control the gain of MESFET amplifiers. In this case, therefore, it is equivalent to having a fourth terminal in the MESFET, highly isolated from the other ports due to the inherent isolation of the optical input. The amount of change in the gain and the time constant associated are functions of the device parameters, the bias conditions, and the input and output matching circuits. These matching circuits are designed using conventional techniques [13], [14] for the FET without illumination.

Measurements of the S-parameters with and without illumination have shown that the device input and output impedance change very little with illumination. Therefore, the dominant effect in the control of the gain is due to the significant change in the transconductance of the device with illumination.

The change in the MESFET equivalent circuit parameters and the correspondent S-parameters are calculated as described in the previous section. The change in the transconductance of the device can also be obtained from the measured S-parameters. Comparisons between the measured and the estimated values of the forward transmission coefficient S_{21} and of the transconductance g_m are made, and good agreement is found. The magnitude of the forward transmission coefficient $|S_{21}|$ and of the transconductance g_{m0} can be varied from ~ 0 to ~ 2.5 and to ~ 40 mS, respectively, when the gate bias voltage is adjusted near the pinchoff and the illumination is increased.

Fig. 9 illustrates the change of the gain of the MESFET amplifier with illumination, when a high ($R_G = 100$ kΩ) resistance is connected to the gate bias circuit. On the horizontal scale is the bias voltage V_{GS} applied to the gate before illumination.

When a low (e.g., $R_G = 1$ kΩ) resistance is connected to the gate bias circuit, the measured gains under illumination and without illumination are very close for any V_{GS} value.

From Fig. 9 it can be observed that up to 20 dB of change in the gain can be obtained when the bias gate voltage V_{GS} is chosen close to the pinchoff voltage ($V_{GS} \sim V_{po}$). Without illumination the device provides a high isolation, (≥ 10 dB) and under illumination the gain is around 10 dB. The rate at which the gain can be changed is basically limited by the product of the gate-to-source capacitance ($C_{gs} \sim 0.5$ pF) with the gate series resistance

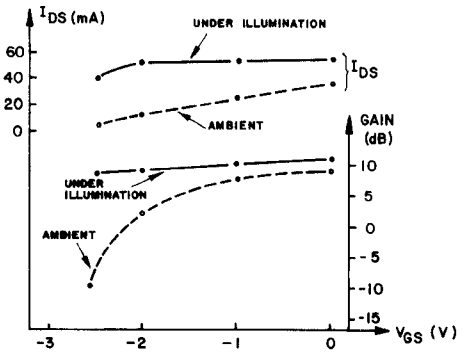

Fig. 9. Change in the gain of the MESFET with illumination ($V_{DS} = 3$ V; $F = 2.8$ GHz; $R_G = 100$ kΩ). V_{GS} is the gate bias voltage as measured before illumination.

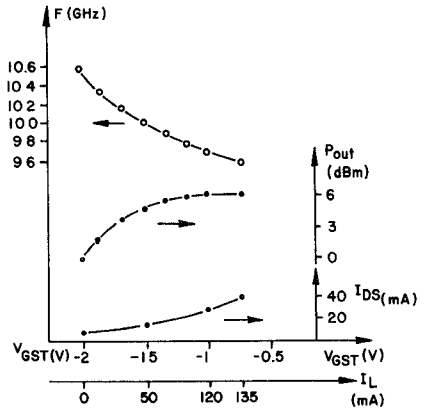

Fig. 10. Measured optical tuning of X-band GaAs MESFET oscillator ($V_{DS} = 2$ V; $V_{GS} = -2$ V).

R_G. For $R_G = 100$ kΩ, $\tau = C_{gs} \cdot R_G \sim 50$ ns which may be adequate in many applications.

Given the small amount of optical power (a few microwatts) needed to control the gain, simple and inexpensive optical sources (such as LED's) can be used to control the gain of FET amplifiers.

V. Optical Tuning of FET Oscillators

Optical techniques where the device is illuminated by a focused laser (or LED) beam can be used to optically tune FET oscillators.

Several configurations can be adopted for the design of FET oscillators, such as using series or shunt feedback and any of the three terminals connected to the ground [6]. One usual configuration is the source series feedback. In this case, the gate circuit being the frequency determining element, the change of the gate-to-source capacitance C_{gs} with illumination has a significant effect in the frequency of oscillation. Then the change in the gate-to-source capacitance C_{gs} has a dominant effect in the tuning of the oscillator. Together with the change in the frequency of oscillation, some variation in the output power may occur. Fig. 10 shows the change in the frequency of operation of a X-band oscillator versus the total voltage $V_{GST} = V_{ph} - V_{GS}$ appearing across the gate and the laser drive current I_L.

These show ~10-percent optical tuning range, the optical absorbed power being a few hundred nanowatts (laser characteristics in Fig. 3). It is shown (Fig. 10) that a reasonable flat output power ($\sim +5$ dBm ± 0.5 dB) is obtained within ~5-percent tuning range. Similar results were obtained using a 2.8-GHz FET oscillator.

Observations in the spectrum show that in some cases the FM noise performance of the FET oscillator can be significantly improved with illumination. The reasons for this improvement are still not well understood. It is a function of the bias point of the FET oscillator, and may well be related to the light effects changing the trapping and detrapping process in different regions of the device.

Given the low optical power involved in the tuning process (~ a few microwatts) it is believed that simple and inexpensive optical sources (such as LED's) could be used with similar results.

VI. Optical Injection Locking of FET Oscillators

Optical injection locking of GaAs MESFET oscillators has recently been observed [15]. Optical injection locking of oscillators in principle is almost identical to electrical injection locking. The only difference is in the way the locking signal is introduced into the oscillator circuit. In the optical approach, the locking signal takes the form of an amplitude modulation of the laser optical carrier which is then coupled into the active region of the FET oscillator. High isolation between output signal and locking signal is obtained due to the inherent isolation of the optical process. However, as it has been mentioned before, for the geometry of the MESFET used, the efficiency of the optical absorption in its active region is poor. Therefore, considering the small optical power absorbed, high locking gains and limited locking ranges are expected. For low injection levels of the locking signal, an approximate analysis gives the following expression for the locking range [6]:

$$2\Delta\omega = \frac{\omega}{Q_i} \cdot \frac{g_m}{\omega C_{gs}} \cdot \frac{|I_L|}{(2P_{\text{out}} \cdot G_L)^{1/2}} \qquad (12)$$

where

- $2\Delta\omega$ locking range,
- ω center frequency,
- Q_i Q of the gate circuit,
- g_m transconductance of the device,
- C_{gs} gate-to-source capacitance,
- I_L locking photocurrent,
- P_{out} free-running output power,
- G_L conductance of the load presented to the FET terminals.

For the typical values used in the experiments (e.g., $g_m \sim 40$ ms, $C_g \sim 0.8$ pF, $P_{\text{out}} \sim 2$ mW, $I_L \sim 10$ μA), (12) gives a locking range around one megahertz, in quite fair agreement with the few MHz locking range found experimentally. For the estimation of the optical power converted in electrical power, a quantum efficiency close to unity is assumed (each absorbed photon produces one electron-hole pair). This has been confirmed by dc measurements [6]. The modulation depths of the optical injected signal are typically in the range 70–90 percent up to around 3 GHz, showing a fast decrease above this frequency [16].

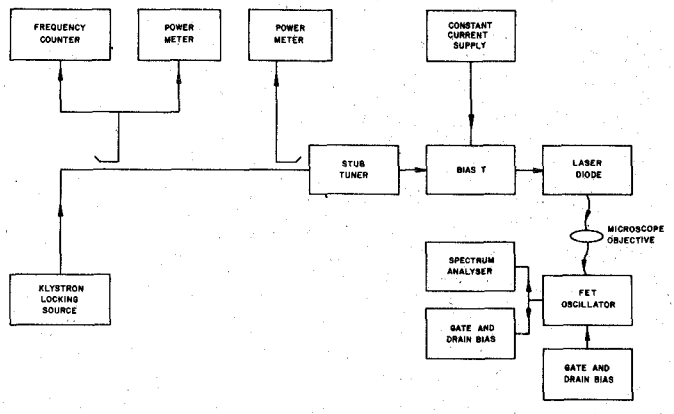

Fig. 11. Block diagram of FET oscillator optical injection-locking experiment.

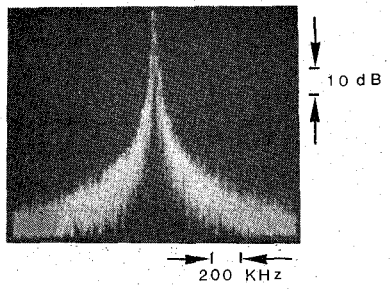

Fig. 12. Spectrum of the free-running FET oscillator ($F_o \sim 2.8$ GHz, $BW = 10$ kHz, $P_{\text{out}} \sim 2$ mW).

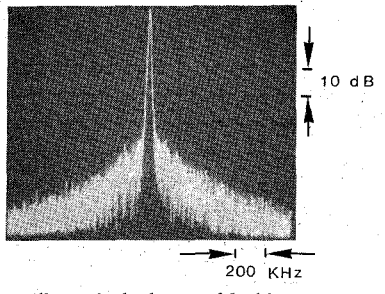

Fig. 13. FET oscillator locked to stable klystron source (same conditions as in Fig. 12).

Fig. 11 illustrates the block diagram of the FET oscillator optical injection locking experiment. As in the previous experiments, a GaAs GAT 6 MESFET from Plessey and a GaAlAs laser diode type LS7709 from ITT were used.

The optical locking performance of the FET was measured by adjusting the laser modulation frequency to a value (~ 2.8 GHz) close to the FET free-running frequency. Fig. 12 shows the free-running FET oscillator ($F_o \sim 2.8$

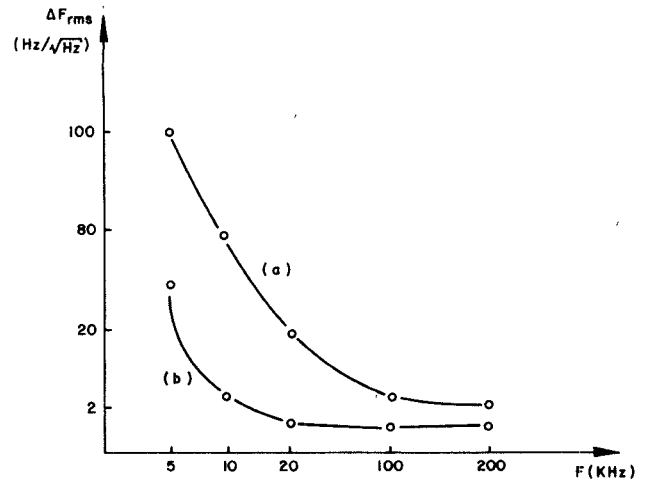

Fig. 14. FM noise of (a) free-running FET oscillator and (b) optically injection locked to the more stable klystron signal.

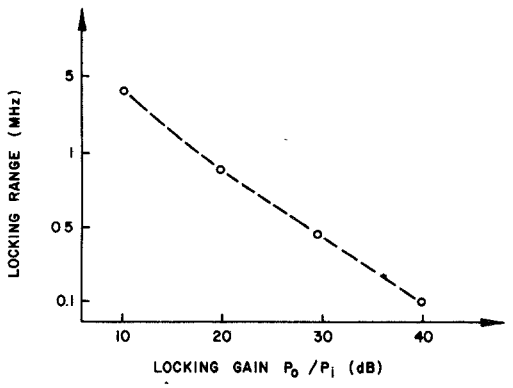

Fig. 15. Optical injection locking characteristics of the FET oscillator.

GHz, $P_o \sim 2$mW); Fig. 13 shows the FET oscillator locked to the laser modulation, so that adjustments of the modulation frequency causes a corresponding shift in the FET oscillator frequency. To ensure that locking was from optical carrier injection and not stray RF leakage, the laser beam was interrupted and it was found that no locking effects would be observed. Conventional electrical injection locking measurements give a loaded Q of around 70 for this oscillator.

Measurements from Fig. 12 indicate [17] an rms FM noise deviation of 80 Hz (1-Hz bandwidth) at 10 kHz from the carrier in accordance with expected performance for free-running FET oscillators which are known to be generally noisy. The locked output FM noise level was substantially reduced, as shown in Fig. 13, to an rms deviation of less than a few hertz at 10 kHz from the carrier. This is to be expected, owing to the superior noise performance of the klystron oscillator to which the FET is locked. Fig. 14 illustrates the reduction of the rms FM noise when the free-running FET oscillator is locked to the more stable klystron signal.

Typical locking ranges were around a few megahertz, in line with (12). Fig. 15 illustrates the locking range $2\Delta f$ versus locking gain (P_o/P_i, dB) obtained experimentally.

The locking range so far achieved could be substantially improved by more efficient coupling of the modulated laser light to the FET chip and by more efficient coupling of the microwave locking signal to the laser chip. The use of a lower Q-factor oscillator circuit could also be of moderate benefit in increasing the locking range. Also, control of the intensity of the optical carrier could be used to pretune the FET oscillator to a frequency close to that of the locking signal. This would provide large operational bandwidths.

The possibility of locking with optical modulation frequencies close to subharmonics of the oscillator frequency is suggested by the inherent nonlinearity of the FET active channel.

VII. Conclusions

Photovoltaic and photoconductive effects in the various regions of the device were considered and the change in the dc and RF characteristics of the MESFET under illumination were predicted. The reduction in the resistivity of the illuminated regions was found to be around 10 percent for the levels of illumination used. However, dramatic changes in the gate depletion width are found when the external gate circuit resistance is high. This requires an external resistance much larger than the internal resistance of the illuminated Schottky barrier acting as a solar cell. Under these conditions, significant changes in the device transconductance and around 20-percent change in the input capacitance are obtained.

The S-parameters estimated from the equivalent circuit parameters with and without illumination are in quite fair agreement with those measured. These are used, together with conventional microwave techniques, to estimate the performance of FET amplifiers and oscillators under illumination. It has been found that when a voltage close to the open-circuit photovoltage of the gate Schottky barrier is allowed to develop, the opening of the FET active channel is pinned to a fixed value. This allows large control of the gain (many decibels) of FET amplifiers and of the frequency (up to 10-percent tuning range) of FET oscillators with a change of a few microwatts of the absorbed optical power. The rate at which the gain and the frequency can be varied is largely limited by the time constant of the gate circuit. Given the low optical power involved in the control of gain and in the tuning process, it is believed that simple and inexpensive optical sources (such as LED's) could be used in several applications where moderate rates of change in those control functions are tolerated.

Optical injection locking of a FET oscillator has been demonstrated. This was first reported in [15]. The experiment used the output of a GaAs/GaAlAs laser diode amplitude modulated at a frequency close to the free-running frequency (~ 2.8 GHz) of the FET oscillator. The noise performance of the FET oscillator is substantially improved, taking on the noise characteristics of the master oscillator to which it is synchronized. A locking range of a few megahertz was obtained. This is in fair agreement with

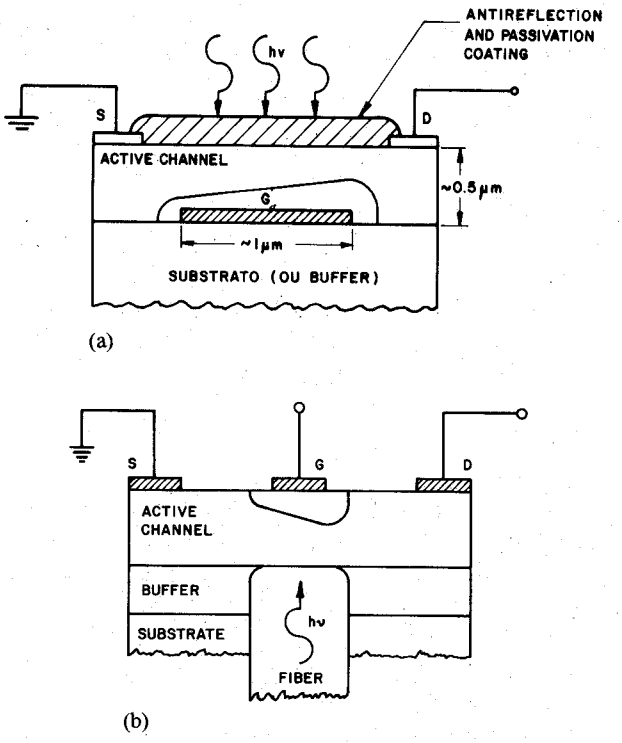

Fig. 16. Two possible alternatives to improve the optical absorption in the active area of the MESFET [6]: (a) buried gate MESFET and (b) illumination from the bottom.

the value predicted by the approximate optical locking equation presented. It is believed that using a suitable structure for optimal optical absorption and pretuning the FET oscillator (by controlling the intensity of the optical carrier) will provide optical locking over bandwidths adequate for practical applications. Fig. 16 (a) and (b) illustrates two possible alternatives to improve the optical absorption in the active area of the MESFET [6].

The possibilities of fabricating these structures need to be closely assessed. Interdigitated-gate FET structures, as those used in power FET's, offer another possibility. These would allow larger absorption surfaces and wider tolerances in the focusing optical system. A diffraction grid could perhaps also be used on the top of the interdigitated structure to redirect the optical energy to the desired regions.

It seems that the first applications of the optical control techniques will be in the area of phased array antennas in which the locking signal could be distributed to individual elements by means of optical fibers, with considerable savings in complexity over conventional systems. An additional advantage of the optical-fiber distribution approach is the low losses associated with the actual single-mode optical fibers.

It can be expected also that the MESFET's will play an important role in the near future in the direct demodulation of high bit-rate optical communication systems and in optical signal processing. Optical techniques may, as well, find considerable importance in GaAs monolithic microwave integrated circuits, where the optical sources, optical guiding structures, and microwave devices can be fabricated in the same chip.

ACKNOWLEDGMENT

Some FET and laser diode samples used in the experimental work were supplied by R. S. Pengelly (Plessey, Caswell) and Dr. G. H. B. Thompson (S. T. L., Harlow), respectively. Many suggestions from Prof. J. R. Forrest are gratefully acknowledged.

REFERENCES

[1] J. Graffeuil, P. Rossel, and H. Martinot, "Light-induced effects in GaAs FETs," *Electron. Lett.*, vol. 15, pp. 439–441, 1979.
[2] J. J. Pan, "GaAs MESFET for high speed optical detection," in *Proc. 22nd SPIE Int. Tech. Symp.* (Monterey, CA), 1978.
[3] C. Baak, G. Elze, and G. Walf, "GaAs MESFET: A high-speed optical detector," *Electron. Lett.*, vol. 13, p. 193, 1977.
[4] J. M. Osterwaller and B. J. Rickett, "GaAs MESFET demodulates gigabit signal rates from GaAlAs injection laser," *Proc. IEEE*, vol. 67, pp. 966–968, 1979.
[5] J. C. Gammel and J. M. Ballantyne, "The OPFET: A new high-speed optical detector," in *Proc. IEDM*, 1978, pp. 120–123.
[6] A. A. de Salles, "Optical control of microwave field effect transistors," Ph.D. thesis, Univ. of London, 1982.
[7] K. Lehovec and R. Zuleeg, "Voltage–current characteristics of GaAs J-FETs in the hot electron range," *Solid-State Electron.*, vol. 13, pp. 1415–1426, 1970.
[8] A. B. Grebene and S. K. Ghandi, "General theory for pinched operation of the junction-gate FET," *Solid-State Electron.*, vol. 12, pp. 573–589, 1969.
[9] R. A. Pucel, H. A. Hans, and H. Statz, "Signal and noise properties of gallium arsenide microwave field-effect transistors," in *Advances in Electronics and Electron Physics*, vol. 38. New York: Academic Press, 1975, pp. 195–265.
[10] A. A. de Salles and J. R. Forrest, "Theory and experiment for the GaAs MESFET under optical illumination," in *Proc. 11th Eur. Microwave Conf.* (Amsterdam), 1981, pp. 280–285.
[11] H. Fukui, "Determination of the basic device parameters of a GaAs MESFET," *Bell Syst. Tech. J.*, vol. 58, pp. 771–797, 1979.
[12] R. A. Minasian, "Simplified GaAs MESFET model to 10 GHz," *Electron. Lett.*, vol. 13, pp. 549–551, 1977.
[13] R. S. Carson, *High Frequency Amplifiers*. New York: Wiley, 1975, p. 151.
[14] R. S. Pengelly, "The design of microwave transistor amplifiers," in *Microwave Solid State Devices and Applications*, M. J. Howes and D. V. Morgan, Eds. London: Peregrinus, 1980.
[15] A. S. de Salles and J. R. Forrest, "Initial observations of optical injection locking of GaAs metal semiconductor field effect transistor oscillators," *Appl. Phys. Lett.*, vol. 38, pp. 392–394, 1981.
[16] A. J. Seeds, "The optical control of avalanche diode oscillators," Ph.D. thesis, Univ. of London, 1980.
[17] S. Hamilton, "FM and AM noise in microwave oscillators," *Microwave J.*, vol. 21, pp. 105–109, 1978.

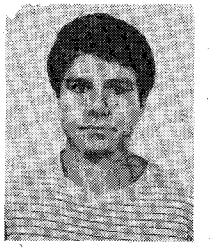

Alvaro Augusto A. De Salles was born in Bagé, RGS, Brazil, on March 6, 1946. He received the B.Sc. degree in electrical engineering from the University of Rio Grande do Sul, Porto Alegre, Brazil, in 1968, the M.Sc. degree in electrical engineering from Catholic University of Rio de Janeiro (PUC/RJ), Brazil, in 1971, and the Ph.D. degree in electrical engineering from University College, London, England, in 1982.

From 1970 to 1978 he worked as an Assistant Professor at the Catholic University Center for Research and Development in Telecommunications (CETUC), in Rio de Janeiro. From 1978 to 1982 he was at University College doing solid-state phased array radar design and research on optical control of GaAs MESFET amplifiers and oscillators. He is now back at CETUC, where he is Head of the Microwave and Optics Group doing research and development on microwave and optical devices for communication and radar. Dr. de Salles is also an Assistant Professor at the Catholic University of Rio de Janeiro.